JOURNAL OF PROPULSION AND POWER
Vol. 22, No. 1, January–February 2006

Microwave Electrothermal Thruster Chamber Temperature Measurements and Performance Calculations

Silvio G. Chianese* and Michael M. Micci†
Pennsylvania State University, University Park, Pennsylvania 16802

The microwave electrothermal thruster (MET) uses microwave frequency energy to create and sustain a resonant cavity plasma to heat a propellant. A 2.45-GHz aluminum cylindrical thruster with converging copper-alloy nozzles was used for this study. A spectroscopic system was used to collect light emitted through a window in the plasma chamber. A Schumann–Runge oxygen-emission model was developed assuming an anharmonically vibrating, nonrigid rotating oxygen molecule. The commercially available LIFBASE software was used to model the ionized molecular nitrogen first negative system emission from the nitrogen plasmas. Experimental data were compared to the temperature-dependent models using least-squared difference summation schemes. Oxygen rotational temperatures of 2000 K and ionized nitrogen rotational temperatures of 5500 K were measured. These measurements were nearly constant for all chamber pressures and investigated absorbed specific powers. CEA2 code equilibrium thermochemical calculations show the relationship among enthalpy addition, temperature, and specific impulse for realistic operating conditions. Nitrogen was found to be an excellent choice as a propellant or propellant component, whereas oxygen was found to be a poor choice because of the temperatures achieved for the respective gases in the MET chamber.

Nomenclature

a	=	cavity radius
f_r	=	resonant frequency
h	=	cavity height
I_{sp}	=	specific impulse
M	=	molecular weight
T_c	=	chamber temperature
ε	=	material permittivity
μ	=	material permeability
χ_{01}	=	first zero of the J_0 Bessel function of the first kind

I. Introduction

THE microwave electrothermal thruster (MET) has been studied under laboratory conditions for more than 20 years. Microwave frequency energy is input into a cylindrical resonant cavity, and a plasma is sustained that heats a propellant that is expanded through a nozzle. Figure 1 shows a schematic of the MET. The device has been successfully operated with several different propellants at a variety of input power levels, propellant flow rates, and chamber pressures. However, to date the true potential performance of the device has not been ascertained. This is due to several factors, including the complex physics involved in the microwave heating, the relatively low thrust of the device, and the difficulty in using conventional diagnostic techniques to study high-temperature molecular plasmas. The objectives of this investigation were to measure the temperature of representative molecular propellants within the device at a variety of operating conditions and to calculate thermochemical and performance parameters at realistic operating conditions. This information can be used to ascertain whether the potential performance of the device is greater than other propulsion systems currently in use.

A. Motivation for Use of the MET

Currently, more than 180 satellites are in use that utilize electric propulsion, and research and development continues in academia, industry, and government laboratories.[1–5] In recent years, the percentage of satellites launched that use some form of electric propulsion for a variety of tasks, from primary propulsion to delicate attitude adjustment, has substantially increased. Several types of electric propulsion systems have been used on operational satellites, and even more have been demonstrated in laboratory experiments. Electrothermal devices, such as the resistojet, arcjet, and MET, are the electric propulsion systems that operate most like conventional chemical rockets. Electromagnetic energy is used to heat a propellant to high temperatures before the gas is expanded through a converging–diverging nozzle.

The major performance difference between chemical and electric propulsion devices is the relatively low thrust and high specific impulse of electric thrusters compared to chemical rockets. For many missions, an I_{sp} greater than that possible from chemical rockets is needed to reduce the propellant mass carried onboard. However, maximizing the I_{sp} is not the only mission constraint. Electric propulsion devices with very high exhaust velocity typically have very low thrust capability because of the large amount of power required to accelerate higher propellant flow rates. This means that spacecraft momentum change is slow, and in some cases not fast enough for the use of such thrusters at all. Therefore, it is desirable for some missions to have a thruster that is capable of specific impulse values greater than chemical rockets while still having relatively high thrust levels. Electrothermal thrusters are devices that can match these criteria.

Resistojets and arcjets have been used on satellites previously. However, both of these systems have performance limitations. Resistojet I_{sp} is limited by the melting temperature of the heating element used. Arcjets do not have this heat transfer limitation. However, because the arc in these systems comes in physical contact with the electrodes, electrode erosion can limit their useful lifetime and makes pulsed operation impossible. In addition, these devices are relatively electrically and thermally inefficient. The microwave electrothermal thruster may operate at a similar thrust and specific impulse as the conventional arcjet with comparable propellant temperatures but potentially offers better practical performance because of better electrical and thermal efficiency and longer useful lifetime.

Received 31 December 2004; revision received 4 May 2005; accepted for publication 30 May 2005.

*Graduate Research Assistant; currently at Northrop Grumman Space Technology, Mailstop 140/2121F Redondo Beach, CA 90254; Silvio.Chianese@ngc.com. Member AIAA.

†Professor, Department of Aerospace Engineering, 229 Hammond Building; micci@psu.edu. Associate Fellow AIAA.

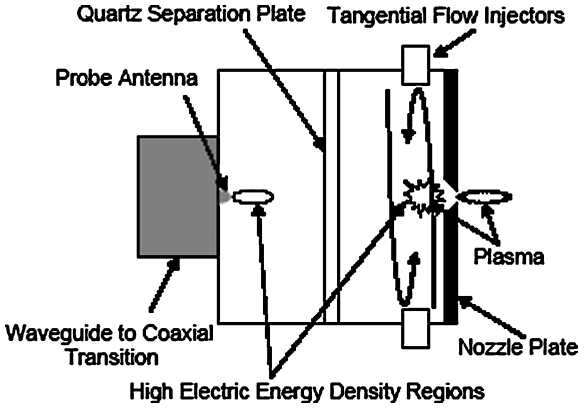

Fig. 1 MET schematic.

B. Microwave Electrothermal Thruster Development

Research on the MET began in the early 1980s at Michigan State University and the Pennsylvania State University.[6,7] This early work focused on proof-of-concept studies and configuration optimization using 2.45-GHz power supplies, which are readily available and relatively inexpensive compared to other microwave frequency supplies. It was during this time period that the transverse magnetic (TM) mode resonant cavity thruster design was selected as the best way to transfer electromagnetic energy into the propellant while isolating the walls of the rocket chamber from the high-temperature plasma. A TM mode is one in which the magnetic-field lines are everywhere perpendicular to the cavity axis. Some early diagnostics work was completed that showed the promise of the device as well as the difficulty in determining the performance of the system. Probes were used to determine that the cavity electrical efficiency was greater than 95% for helium and nitrogen discharges from 4.0 to 133.3 kPa. Spectroscopic techniques were employed that were able to estimate electronic temperatures on the order of 10,000 K with some confidence. However, determination of heavy particle translational temperature proved elusive. Early versions of the MET required active impedance matching to improve performance characteristics. However, operation with very high electrical efficiency ($> 98\%$ input microwave power absorbed) was demonstrated for a system with a fixed geometry and input power between 1.4 and 2.2 kW using helium and nitrogen as propellants.[8] Electrical efficiency of the MET is typically measured by comparing the power that is input into the cavity to the power that is reflected. Spectroscopic measurements conducted with helium plasmas showed electronic temperatures between 10,200 and 10,900 K for medium power testing (200–400 W) and between 12,000 and 12,800 K for high power (750–2150 W) testing.[9,10] These measurements were insensitive to operating conditions such as flow rates (0–83.2 mg/s) and chamber pressures (30–270 kPa). These measurements were for spatially averaged temperatures. However, spatially resolved emission spectroscopy has shown the radial profile of the helium electronic temperature has a maximum of approximately 12,000 K in the center of the plasma and decreases to about 11,000 K at the edge of the plasma.[11] These results were also insensitive to operating power (500–1000 W) and chamber pressure (125–250 kPa).

In the late 1990s a significant research effort was initiated to explore the use of the MET at low powers (< 100 W).[12–14] This effort demonstrated that the device could be operated at 7.50 GHz with excellent electrical efficiency ($> 98\%$ input microwave power absorbed) with helium, nitrogen, and ammonia as propellants with as low as 65 W of input power. The mean chamber temperature of the heavy particles was experimentally determined as a function of input specific power by measuring chamber pressure and flow rate. The maximum mean chamber temperatures realized were 1700, 2100, and 1200 K for helium, nitrogen, and ammonia, respectively. Helium electronic temperature measurements were made with a relative line intensity method using four different spectral line intensity ratios at three different operating pressures, 193.1, 255.1, and 344.7 kPa. As the pressure increased, the temperatures measured from each ratio approached a self-consistent value of approximately 4000 K ($\pm 18\%$). Doppler-shift experiments were conducted to determine the helium propellant centerline specific impulse from the MET as a function of specific power, with an absolute input power of 80 W. The centerline specific impulse increased with specific power, with a maximum measured value of approximately 1300 s at a specific power of 30 MJ/kg.

Researchers in industry have begun to develop MET laboratory studies as well. Investigators at the Aerospace Corporation have recently completed a study on the use of water vapor as a propellant for the MET.[15,16] For this work, a momentum trap thrust stand was used with a power supply that was tunable from 2.1 to 4.1 kW with 80–100% input power absorbed by the water plasma in the chamber. A maximum thrust value of 250 mN was measured, and a maximum specific impulse of 428 s was calculated from the knowledge of propellant flow rates and thrust values. These values compare favorably to conventional hypergolic chemical rockets used for satellite propulsion. Investigators at Research Support Instruments have begun studying the use of the MET operating with helium and nitrous oxide as propellants with 150 W of input power.[17] A pendulum-based thrust stand was used to measure the thrust from the device while it was operating in a horizontal orientation. Buoyancy effects have precluded accurate performance measurements for most operating conditions to date. However, a helium propellant thrust up to 50 mN and specific impulse up to 350 s were measured. Nitrous oxide propellant thrust of more than 70 mN and specific impulse of more than 170 s were measured.

In addition to the experimental studies undertaken, several computational investigations have been conducted to analyze the MET. Initial studies considered only a single-temperature model with helium as the propellant.[18] This work showed qualitatively the strong fluid-dynamic control over plasma location. More recent work incorporated a two-temperature model to examine the helium plasma flow.[19] A fully coupled fluid-dynamic Navier–Stokes and electromagnetic Maxwell equations model was used. The plasma was found to be highly nonequilibrium in nature with electron and heavy-particle temperatures that differ greatly. A calculation with 4 kW of input power and 220 mg/s of propellant flow was found to have a thrust of 0.721 N and an I_{sp} of 334 s. Although the modeling effort is encouraging, the fluid flow modeled was not similar to that used in experimental investigations and 1.1 kW of the input energy flowed out of the thruster calculation domain through a nonrealistic pathway. In addition, the calculations suggested that maximum propellant heating did not occur on the plasma centerline, as found experimentally.

C. Research Motivation and Objective

Previous experimental studies of the microwave electrothermal thruster have shown that it can be operated at high electrical efficiency over a variety of power ranges and flow rates with several different propellants. One way to assess the potential performance of a thermal rocket is to measure the temperature of the gas in the chamber. Knowledge of the temperature gives a measure of the potential specific impulse of the rocket for a given operating condition:

$$I_{sp} \propto \sqrt{T_c/\bar{M}} \tag{1}$$

Measuring the temperature in the plasma chamber of a MET is not a simple matter. The high-temperature free-floating plasma surrounded by tangentially injected propellant potentially creates a strong temperature gradient within the chamber. This, along with the electromagnetic energy present in the chamber, makes use of thermocouples or other probes unfeasible. The plasma emits a significant amount of light over a broad spectrum when molecular propellants are used. Without careful consideration, this light emission would cause interference with typical laser-based thermometry measurements, such as laser-induced fluorescence (LIF) and spontaneous Raman scattering spectroscopy. In addition, there can be several different molecular temperatures corresponding to the different energy storage modes in molecules.

Using spatially resolved molecular-emission spectroscopy with a quantum-mechanical and statistical-thermodynamics model, it is possible to determine the molecular rotational, and thus translational, temperature within the MET plasma chamber. Molecular rotational and translational temperatures are assumed to be the same because of the very fast equilibration between the two types of energy storage at the pressures of interest in this investigation. The physical processes by which the microwave energy is transferred to the gas molecules and the properties of potential propellants at elevated temperatures have not been investigated in the past but are of critical importance in propellant selection and performance evaluation. The first objective of this investigation was to determine and compare the spatially resolved rotational temperature of representative molecular propellants, oxygen and nitrogen, in the MET plasma chamber while varying the chamber pressure and absorbed specific power independently. These fluids could potentially be used as MET propellants themselves, and they are also components of more complex liquid storable propellants. The thermochemical and structural properties of these of oxygen and nitrogen are well known, making temperature-dependent spectroscopic modeling feasible. The second objective was to calculate chamber thermochemical properties and the potential performance of the thruster operating with representative propellants at realistic operating conditions.

II. MET Theory

The electromagnetic field distributions within the MET cavity can be found by solving Maxwell's equations for a closed cylindrical cavity with perfectly conducting walls.[20,21] A transverse magnetic (TM) mode of resonance is used to create maximum electric-energy density along the axis at the two ends of the cavity. The TM_{mnp} modes have no magnetic fields along the axial direction and have m full-period variations of the electric field along the circumferential direction, n half-period variations in the radial direction, and p half-period variations along the cavity length. The TM_{011} mode was chosen to create maximum electric-energy density regions near the thruster nozzle and the antenna coupler along the cavity centerline, with plasma formation forced to occur at the nozzle end. Figure 2 shows the variation of the instantaneous electric-energy density in a plane along the cavity axis for a 15.75-cm-long thruster with a 10.16-cm diam. The resonant frequency of a cavity can be found as a function of the cavity height and radius:

$$(f_r)_{011}^{\mathrm{TM}} = \left(1/2\pi\sqrt{\mu\varepsilon}\right)\sqrt{(\chi_{01}/a)^2 + (\pi/h)^2} \qquad (2)$$

The first step in creating stable resonant cavity microwave plasmas is to create free electrons in the ambient gas by initiating gaseous breakdown in a vacuum. Once breakdown occurs, and a small number of electrons are released into the gaseous mixture, a much larger number of free electrons can be released through electron impact ionization.[22] After a plasma has been initiated, free electrons continue to absorb energy from the electric field and distribute some of that energy throughout the gas via collisions with heavy particles. The fraction of the absorbed energy that is passed from electrons to heavy particles and in what manner the energy is transferred is a function of both the heavy-particle characteristics and the particular electron-energy distribution.[23–25] As propellant is injected into the plasma chamber after the initial near-vacuum diffuse plasma is formed, the plasma coalesces into a rotating teardrop-shaped structure as the chamber pressure rises. For microwave frequency molecular plasmas at atmospheric pressure, the energy exchange is often assumed to be equilibrium in nature, with Joule heating as the energy-transfer mechanism. A review of the literature shows that the electronic excitation temperature, usually found from a seed metal, and the molecular rotational temperature are similar, but typically vary by 500–1000 K.[26–30]

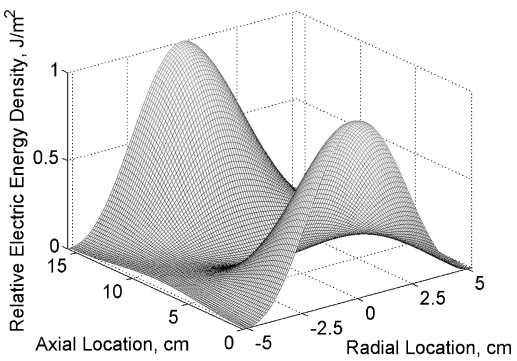

Fig. 2 Instantaneous electric energy distribution for TM_{011} cavity.

Local thermodynamic equilibrium (LTE) is often assumed in these situations. The transition from nonequilibrium diffuse plasma to near-LTE conditions in a contracted plasma is known as a glow-to-arc transition, which is characterized by an increase in plasma current density.[31] The plasma contraction in the MET is indicative of a change from a nonequilibrium state toward LTE. However, contraction of the plasma is not in itself confirmation of LTE, because nonequilibrium can persist in resonant cavity plasmas even with plasma contraction.[32] Although an assumption of thermal equilibrium may be appropriate for some devices, a relatively small change in measured temperature can mean a significant change in thermal-rocket calculated performance. For example, a change in measured nitrogen rotational temperature from 5000 to 6000 K would mean a calculated increase of approximately 10% in I_{sp}. Therefore, it is necessary to measure the heavy-particle rotational temperature directly, rather than the excitation temperature of a seed metal. This noted deviation from thermal equilibrium is due to the electron impact excitation and deactivation of molecular internal-energy storage modes. The thermochemical differences between particular propellants also have an effect on the heating process and potential thruster performance. The thermal conductivity, dissociation energy, and equilibrium enthalpy of a propellant all influence the final thermochemical state of a propellant heated by the microwave energy. These properties and the potential performance of the MET can be compared using the CEA2 code developed by researchers at NASA Glenn Research Center.[33,34] Data calculated using CEA2 are presented in Sec. V.

III. Experimental Apparatus and Procedures

A. Apparatus

Microwave power is produced by a Gerling Laboratories model GL103 low-ripple power supply connected to a model GL131, 2.45-GHz magnetron. The microwave output of the system can be tuned from 0 to 2.2 kW. Microwave energy is sent from the magnetron via waveguide through a three-port circulator and dual-directional coupler to a coaxial input into the resonant cavity. A 2.06-cm-diam copper hemispherical probe antenna is used to input energy into the cavity. The Gerling GL401A three-port circulator is used to direct power reflected back from the plasma onto a water-cooled dummy load to protect the magnetron. Water also flows around the magnetron to absorb waste heat. The Gerling dual-directional coupler is used to sample the forward and reflected power, and Hewlett-Packard model 478A thermistor mounts and model 432A power meters are used to measure these powers. The power-measurement system has a measurement uncertainty of ± 36 W for forward power measurement and ± 11 W for reflected power measurement.

Equation (2) governs the combinations of cavity length and radius that can be used to create resonance for the TM_{011} mode. To minimize a toroidal region of high electric-energy density present near the midplane of the cavity, a cavity with a relatively small radius is preferred. The 15.75-cm-long, 10.16-cm-diam cavity shown schematically in Fig. 1 is constructed of aluminum with a copper-alloy nozzle insert located at the center of one end. The exhaust gases pass through a conical converging nozzle with a 60-deg cone angle. Nozzles with throat diameters of 0.813, 1.016, and 1.295 mm were used. The cavity is divided into two chambers, a plasma chamber and an antenna chamber, by a 6.35-mm-thick quartz separation plate. The circular plate is nearly transparent to microwave frequency energy, but it can seal the antenna chamber from the injected gas. This forces plasma formation to occur only in the plasma chamber,

closest to the nozzle, where the pressure is lower, thus preventing antenna erosion and preferentially heating the exhaust gasses. There are three equally spaced 0.355-mm-diam tangential flow injectors located 2.54 cm below the nozzle plate used for nearly all spectroscopic testing. These injectors help ensure the plasma is located in a low-pressure region along the cavity axis by creating vortical flow. There is a 5.1-cm-diam viewing window in the side of the plasma chamber that allows for optical confirmation of plasma formation and spectroscopic investigations. The window is placed over a grid of 2.0-mm-diam holes spaced 5.56 mm apart in the side of the chamber that prevents microwave leakage. A pressure port is located along the chamber wall of the plasma chamber and an Omegadyne model PX41T0 pressure transducer was used to measure pressure. The transducer has a measurement uncertainty of ± 0.86 kPa. Figure 3 shows a picture of the MET.

UNIT Instruments mass flow controllers (MFC) model UFC-8100 was used to regulate the mass flow of gasses. The controller has a regulation uncertainty of ± 0.2 mg/s. To initiate plasmas, the pressure in the plasma chamber must be lowered using a vacuum pump until a large-enough electric-field-strength-to-pressure ratio is attained. The pump used is capable of lowering the pressure in the plasma chamber to approximately 690 Pa.

To complete the spectroscopic studies, it was necessary to determine the intensity of light emitted over a range of wavelengths. The optical setup used is shown schematically in Fig. 4. The light given off by the chamber plasma exits the viewing window and enters a 12.7-cm-long tube with a 6.35-mm inner diameter. This probe attachment is placed on two mechanical traverses, one with lateral control and one with vertical control. This allows for controlled spectroscopic investigation of different spatial locations within the plasma chamber. The probe is connected to a fiber-optic cable input. After passing through the fiber-optic cable, the light is collimated and then focused through the opening slit of a SPEX 1870 spectrometer and onto the diffraction grating. The spectrometer has a 0.5-m, f/6.9 Czerney–Turner system with a Bausch and Lomb 2400-lines/mm-ruled diffraction grating, blazed at 3000 Å. The light is then passed through a second slit onto a Hamamatsu model 1P28A photomultiplier tube (PMT). A Pacific Instruments model 126 photometer and AD-126 amplifier/discriminator convert the photon counts to an analog signal and amplify it.

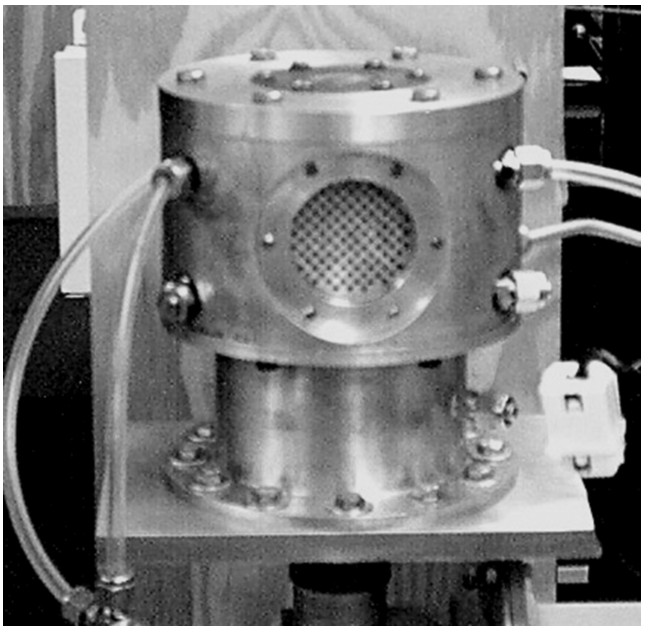

Fig. 3 MET system. Resonant cavity diameter is 10.16 cm; length is 15.75 cm.

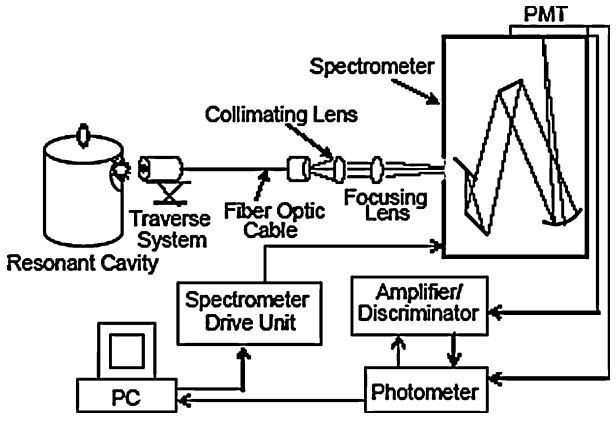

Fig. 4 Spectroscopic system schematic.

B. Procedures

To form plasmas in the MET plasma chamber, propellant gas is first injected through the chamber for several minutes to ensure that only the desired gas is present in the chamber and feed lines. Then, the vacuum pump is used to lower the chamber pressure to approximately 1.38 kPa. The magnetron power is turned on at a relatively low setting of approximately 500 W and slowly increased. Immediately, diffuse plasma spreads throughout the plasma chamber. Mass flow into the chamber is initiated through the tangential injectors at the desired flow rate for the test. As gas accumulates in the chamber and the pressure rises, the plasma's appearance changes. The plasma contracts into a rotating teardrop-shaped structure and becomes brighter. Once the pressure inside the chamber reaches atmospheric pressure, the vacuum cap covering the exhaust nozzle is removed. The chamber pressure continues to rise for approximately 1 min. The final pressure value is dependent upon the mass flow rate, absorbed power, nozzle throat diameter, and propellant in use. For spectroscopic testing, the mechanical traverse system is adjusted so that the column of light is collected from the desired location. After the chamber pressure stabilizes, a spectroscopic emission scan is completed. The data collection lasts approximately 3 min for each scan. Oxygen plasmas were scanned over the 3500–3750 Å range, in 0.10-Å increments, and nitrogen plasmas were scanned over the 3885–3917 Å range in 0.02-Å increments.

IV. Spectral Models

A model was developed for this investigation to predict the temperature-dependent Schumann–Runge oxygen-emission spectrum. For this model, the molecular state energies were determined assuming an anharmonically vibrating, nonrigid rotating molecule.[35,36] Electronic, vibrational, and rotational initial and final state constants were taken from reference sources.[37,38] Transitions between some initial states to some final states are not quantum mechanically allowable within the electronic transition for the Schumann–Runge system. All vibrational transitions, $\Delta v = 0, \pm 1, \pm 2, \pm 3, \ldots$ can occur. However, rotational transitions are limited to the P branch ($\Delta J = -1$) and the R branch ($\Delta J = +1$). Also, rotational transitions are only allowed to final states with odd rotational quantum numbers. For each allowable rotational transition, there is a triplet system of emission lines because of electron spin splitting. Each of these triplet lines has a different transition probability, and the probabilities differ for the P and R branch. For each branch, the rotational transition probability for each transition is the sum of triplet transition probabilities, which are solved for analytically. The electronic and vibrational transition probabilities have been calculated for earlier studies, and are available in the literature. Vibrational transitions are considered for $v' = 0, 1, 2, \ldots, 12$ and $v'' = 0, 1, 2, \ldots, 30$, with 115 P and R branch transitions in each vibrational band. The vibrational and rotational population distributions in the excited state were calculated as a function of temperature assuming a Boltzmann distribution. A triangular instrumental line shape was modeled with a spectral line full width at half maximum intensity (FWHM) corresponding to that found experimentally.

To determine the temperature in the chamber plasma, a method to compare the experimental spectra to the theoretical spectra was

devised. Four relatively intense peaks ($\lambda = 3551.8$ Å, 3594.3 Å, 3629.5 Å, 3722.5 Å) resulting from molecules in the vibrational ground state were identified. The different ratios of the intensities of the peaks were calculated from 1000 to 2500 K, in 25-K increments. The use of multiple ratios reduces the overall error introduced by small measurement or modeling errors of individual peaks or ratios. A simple code was written to extract the relative intensities and relevant ratios of the four peaks considered from each spectral scan. To determine the temperature of the chamber plasmas, the experimentally measured peak-intensity ratios were compared to the modeled peak-intensity ratios. This was done using a least-squared-difference summation scheme. The squared difference between the experimental ratios and modeled ratios was summed for each of the ratios and the temperature with the minimum value of squared-differences summation was the determined temperature.

The commercially available LIFBASE spectral-simulation software was used to model the N_2^+ first-negative-system (FNS) emission spectrum.[39] This is a transition from the $B^2\Sigma_u^+$ excited state to the $X^2\Sigma_g^+$ ground electronic state of N_2^+, which is often evident in pure nitrogen plasmas. The particular transition band studied was the $v' = v'' = 0$ transition. This was chosen because it is a relatively intense transition band that has many rotational transitions that do not overlap with transitions from other vibrational bands. The N_2^+ rotational temperature is assumed to be the same as the neutral heavy-particle rotational and translational temperature because of the few collisions needed for equilibration of rotational and translational energy. A database of modeled spectra from 3821 to 3918 Å was created in 0.02-Å increments in temperature intervals of 100 K from 3000 to 9000 K. The relative simplicity of the N_2^+ FNS emission spectrum over the wavelength range investigated allows for a complete comparison between the spectral model and experimental data. The squared difference between every experimental data point and the corresponding LIFBASE modeled intensity was calculated as a function of temperature from 3000 to 9000 K in 100-K increments, except for the region between 3896.3 and 3898.0 Å. In this region, there was absorption of the plasma emission by the optical components used. The chamber temperature was determined when the summation of the squared differences was minimized.

V. Results

A. Emission Thermometry

More detailed descriptions of these spectral models and results of the separate oxygen and nitrogen spectroscopic investigations can be found in other publications by the authors.[40,41] The principal results are presented here for comparison purposes. There was no spatial variation in measured temperature for either the oxygen or nitrogen plasmas for any operating conditions considered. The following results presented are temperature measurements made transverse to the cavity centerline, 1.9 cm upstream of the nozzle entrance. Figure 5 shows the variation of temperature with pressure for an oxygen propellant flow rate of 69.75 mg/s with an input power of approximately 1.4 kW, resulting in a specific absorbed power of 20.1 MJ/kg.

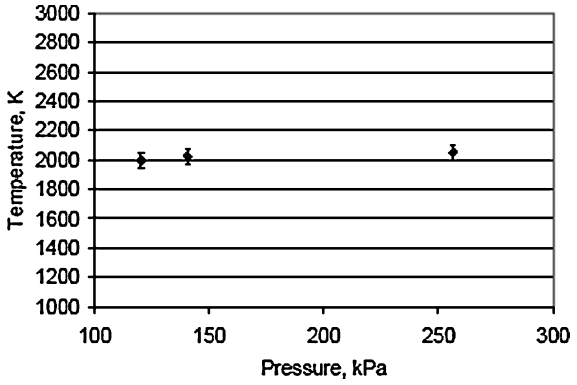

Fig. 5 O_2 rotational temperature vs pressure for a specific absorbed power of 20.1 MJ/kg.

The different pressures were achieved by the use of the 0.813-mm-, 1.016-mm-, and 1.295-mm-diam nozzles for these tests. The bars indicate one standard deviation (±53.7 K) in measured temperature. This figure suggests that the oxygen plasma temperature measured in the chamber of approximately 2000 K does not change with varying pressure, within the testing resolution. This means that either the plasma is already in thermal equilibrium or that the collisional rate increase at higher pressures is ineffective in bringing the system closer to thermal equilibrium over this pressure range.

Figure 6 shows the variation of oxygen rotational temperature with specific absorbed power at a constant chamber pressure of approximately 117.2 kPa and a flow rate of 23.3 mg/s. The absorbed power was varied from 1.12 to 1.61 kW for these tests. It appears there may be a slight increase in chamber temperature as the specific power increases, with a minimum temperature near 1800 K at a specific absorbed power of 48.1 MJ/kg and a maximum measured temperature near 1930 K at a specific absorbed power of 69.5 MJ/kg. This is most likely due to the increase in energy available per molecule. The temperature is not a strong function of specific power, however. The plasma appears to swell in volume as the specific power is increased. Therefore, it is surmised that most of the additional energy added goes to heating a larger volume of gas to a certain temperature, rather than increasing the maximum temperature in the chamber.

Figure 7 shows the variation in ionized nitrogen rotational temperature with chamber pressure for three different specific absorbed powers. For these tests, propellant flow rate was varied from 46.9 to 93.8 mg/s, with a nearly constant absorbed power, 1.05–1.10 kW. The bars represent one standard deviation (±158 K) in measured temperature. The measured temperature of approximately 5500 K does not appear to vary significantly with either pressure or specific absorbed power for these conditions. The different pressures were achieved by the use of the 0.813-mm-, 1.016-mm-, and 1.295-mm-diam nozzles for these tests as well.

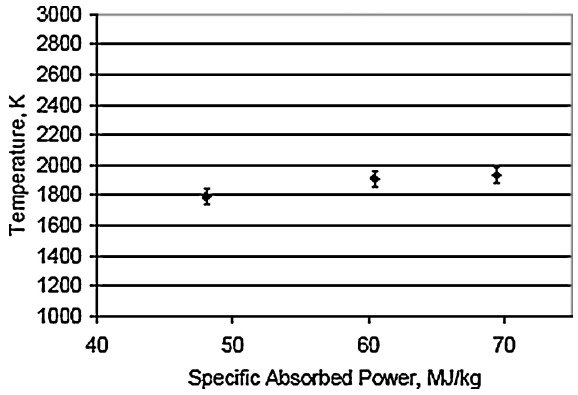

Fig. 6 O_2 rotational temperature vs specific absorbed power at 117.2 kPa.

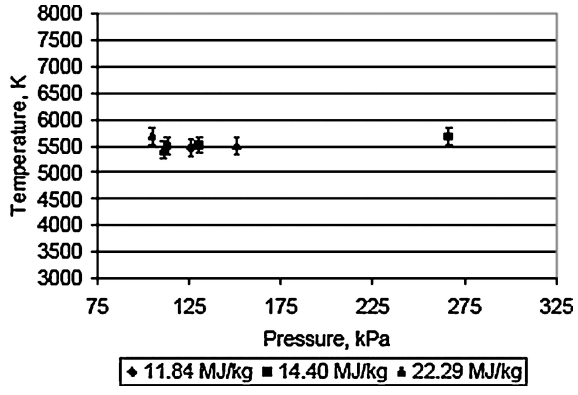

Fig. 7 Variation in N_2^+ rotational temperature vs chamber pressure.

B. Thermochemical and Performance Calculations

The NASA Glenn Research Center–developed CEA2 code[33,34] was used to calculate equilibrium thermochemical properties and performance for MET propellants. In addition to oxygen and nitrogen, ammonia was analyzed because it is a liquid storable propellant that has been demonstrated as a MET propellant. The results of the calculations give a good measure of the potential maximum performance of the MET for a given chamber temperature. Figure 8 shows the equilibrium enthalpy addition needed to raise the propellants from the zero enthalpy condition at standard temperature and pressure to a given temperature at 202.65 kPa of pressure. For all temperatures, the ammonia requires a larger equilibrium enthalpy addition, because of the energy needed for dissociation of the propellant into molecular hydrogen and nitrogen. The enthalpy needed rises faster for ammonia than the other propellants because at the temperatures shown, much of the enthalpy addition is used to dissociate the molecular hydrogen. For temperatures up to 3000 K, the equilibrium enthalpy addition needed for oxygen and nitrogen is very similar. For higher temperatures, oxygen requires a significantly larger enthalpy increase because of dissociation losses. For example, to heat the propellants to 5000 K under equilibrium conditions would require the enthalpy addition of 6.4 MJ/kg for nitrogen, 20.6 MJ/kg for oxygen, and 58.4 MJ/kg for ammonia. There are significant differences between the measured temperatures presented in Sec. V.A for a given specific absorbed power and calculated temperatures for a given equilibrium enthalpy addition shown in Fig. 8. It appears that as specific absorbed power was increased during testing, a larger number of gas molecules were heated to the measured temperatures, rather than a given number of molecules being heated to higher temperatures approaching equilibrium values.

Figure 9 shows a comparison of the chamber propellant equilibrium enthalpy vs I_{sp} for a chamber pressure of 202.65 kPa and a nozzle expansion ratio of 250 with equilibrium chemistry. For enthalpy of less than 35 MJ/kg, nitrogen propellant has a better I_{sp} than oxygen. Even though ammonia propellant has a large enthalpy

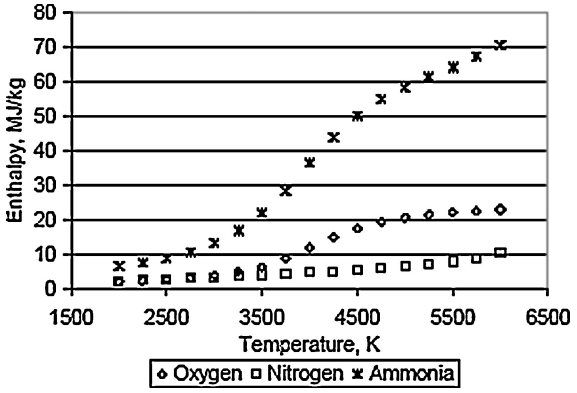

Fig. 8 Calculated equilibrium enthalpy addition vs temperature.

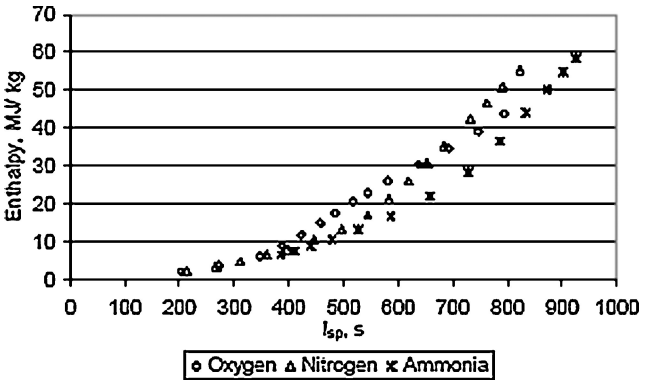

Fig. 9 Calculated equilibrium enthalpy vs I_{sp} for O_2, N_2, and NH_3.

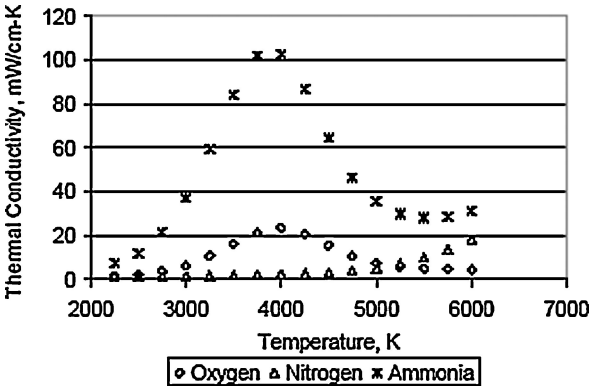

Fig. 10 Calculated equilibrium thermal conductivity for O_2, N_2, and NH_3.

loss to dissociation, it still can achieve a greater I_{sp} than oxygen or nitrogen at any given enthalpy because of the low molecular weight of the gas mixture resulting from dissociation of the ammonia. For example, an equilibrium enthalpy of 20 MJ/kg results in an I_{sp} of approximately 510 s for oxygen, 570 s for nitrogen, and 640 s for ammonia.

Figure 10 shows the temperature-dependent equilibrium thermal conductivity of oxygen, nitrogen, and ammonia at a pressure of 202.65 kPa. For comparison, dry air at 1 atm of pressure has a thermal conductivity of 0.24 mW/cm · K and aluminum has a thermal conductivity of 2050 mW/cm · K. The propellant gas in the MET chamber can be up to two orders of magnitude more thermally conductive than dry air. Gas thermal conductivity is also a function of pressure, but the temperature dependence is more pronounced. A relatively high thermal conductivity can assist the energy transfer from the high-temperature plasma to the surrounding gas. However, not all the energy that is input into the MET plasma will be absorbed and used to increase the enthalpy of the flow exiting the nozzle. Some of the energy will be lost by conduction through the plasma and gas to the walls of the chamber.

VI. Conclusion

The heavy-particle translational temperatures measured, 2000 K and 5500 K for oxygen and nitrogen respectively, were nearly constant for all operating conditions. These temperatures are below equilibrium levels for the specific absorbed powers employed during testing. Assuming the gas exhausted through the nozzle is heated to the same temperature as measured for the plasma in the chamber, neglecting losses due to thermal conduction and radiation to the walls and nonequilibrium chemistry, a specific impulse of 205 s could be achieved with oxygen as the propellant and 395 s with nitrogen. The oxygen does not get hot enough for use as an effective thermal rocket propellant. The nitrogen I_{sp} is above that seen for practical bipropellant rockets. Oxygen and nitrogen are found as components of many other potential liquid storable propellants. The results of this investigation lead to the conclusion that having oxygen in a propellant gas mixture will not lead to having high chamber temperatures, whereas the presence of nitrogen may do so. For example, if the nitrogen present in thermally decomposed ammonia is heated to 5000 K and can collisionally heat the rest of the gas mixture to the same temperature, the potential maximum specific impulse would be approximately 925 s, neglecting losses. Even with significant losses the specific impulse would be better than conventional chemical thrusters. The performance with other nitrogen-containing mixtures also may be good. For example hydrazine exothermally decomposes into a mixture containing nitrogen, and so there would be no energy loss for the initial decomposition, with the additional energy used to heat the mixture to even higher temperatures. The results of this investigation suggest that research should continue on the MET, focusing now on measuring and optimizing actual performance parameters, such as thrust and specific impulse, with practical propellants.

Acknowledgments

This research was funded by NASA Marshall Space Flight Center Grant NGT08-52925 through the Graduate Student Researcher Program.

References

[1]Dunning, J., Jr., Hamley, J., Jankovsky, R., and Oleson, S., "An Overview of Electric Propulsion Activities at NASA," AIAA Paper 2004-3328, July 2004.

[2]Saccoccia, G., "Electric Propulsion in ESA," AIAA Paper 2004-3329, July 2004.

[3]Tverdokhlebov, S., "Overview of Electric Propulsion Activities in Russia," AIAA Paper 2004-3330, July 2004.

[4]Myers, R., "Overview of Major U.S. Industrial Electric Propulsion Programs," AIAA Paper 2004-3331, July 2004.

[5]King, B., "Review of the EP Activities of U.S. Academia," AIAA Paper 2004-3332, July 2004.

[6]Micci, M. M., "Prospects for Microwave Heated Propulsion," AIAA Paper 84-1390, June 1984.

[7]Hawley, M. C., Asmussen, J., Filpus, J., Whitehair, S., Hoekstra, C., Morin, T., and Chapman, R., "Review of Research and Development on the Microwave Electrothermal Thruster," *Journal of Propulsion*, Vol. 5, No. 6, 1989, pp. 703–712.

[8]Sullivan, D., and Micci, M., "Performance Testing and Exhaust Plume Characterization of the Microwave Arcjet Thruster," AIAA Paper 94-3127, June 1994.

[9]Balaam, P., and Micci, M., "Investigation of Free-Floating Resonant Cavity Microwave Plasmas for Propulsion," *Journal of Propulsion*, Vol. 8, No. 1, 1992, pp. 103–109.

[10]Mueller, J., and Micci, M., "Microwave Waveguide Helium Plasmas for Electrothermal Propulsion," *Journal of Propulsion and Power*, Vol. 8, No. 5, 1992, pp. 1017–1022.

[11]Balaam, P., and Micci, M., "Investigation of Stabilized Resonant Cavity Microwave Plasmas for Propulsion," *Journal of Propulsion and Power*, Vol. 11, No. 5, 1995, pp. 1021–1027.

[12]Nordling, D., Souliez, F., and Micci, M., "Low-Power Microwave Arcjet Testing," AIAA Paper 98-3499, July 1998.

[13]Souliez, F., Chianese, S., Dizac, G., and Micci, M., "Low-Power Microwave Arcjet Testing: Plasma and Plume Diagnostics and Performance Evaluation," AIAA Paper 99-2717, June 1999.

[14]Souliez, F., "Low-Power Microwave Arcjet Spectroscopic Diagnostics and Performance Evaluation," M.S. Thesis, Dept. of Aerospace Engineering, Pennsylvania State Univ., University Park, PA, 1999.

[15]Diamant, K., Brandenburg, J., Cohen, R., and Kline, J., "Performance Measurements of a Water-Fed Microwave Electrothermal Thruster," AIAA Paper 2001-3900, July 2001.

[16]Diamant, K., Cohen, R., and Brandenburg, J., "Tunable High-Power Microwave Electrothermal Thruster Performance on Water," AIAA Paper 2002-3662, July 2002.

[17]Sullivan, D., Kline, J., Zaidi, S., and Miles, R., "A 300-W Microwave Thruster Design and Performance Testing," AIAA Paper 2004-4122, July 2004.

[18]Venkateswaran, S., Merkle, C., and Micci, M., "Analytical Modeling of Microwave Absorption in a Flowing Gas," AIAA Paper 90-1611, June 1990.

[19]Chiravalle, Y., Miles, R., and Choueiri, E., "A Non-Equilibrium Numerical Study of a Microwave Electrothermal Thruster," AIAA Paper 2002-3663, July 2002.

[20]Balanis, C., *Advanced Engineering Electromagnetics*, Wiley, New York, 1989.

[21]Chan, T. C. T. V., and Reader, H. C., *Understanding Microwave Heating Cavities*, Artech House, Boston, 2000.

[22]Nasser, E., *Fundamentals of Gaseous Ionization and Plasma Electronics*, Wiley, New York, 1971

[23]Capitelli, M., Ferreira, C., Gordiets, B., and Osipov, A., *Plasma Kinetics in Atmospheric Gases*, Springer, Berlin, 2000.

[24]Biberman, L., Vorob'ev, V., and Yakubov, I., *Kinetics of Nonequilibrium Low-Temperature Plasmas*, Consultants Bureau, New York, 1987.

[25]Fridman, A., and Kennedy, L., *Plasma Physics and Engineering*, Taylor and Francis, New York, 2004.

[26]Raizer, Y., *Gas Discharge Physics*, Springer-Verlag, Berlin, 1991.

[27]Ogura, K., Yamada, H., Sato, Y., and Okamoto, Y., "Excitation Temperature in High-Power Nitrogen Microwave-Induced Plasma at Atmospheric Pressure," *Applied Spectroscopy*, Vol. 51, No. 10, 1997, pp. 1496–1499.

[28]Hadidi, K., Woskov, P., Flores, G., Green, K., and Thomas, P., "Effect of Oxygen Concentration on the Detection of Mercury in an Atmospheric Microwave Discharge," *Japanese Journal of Applied Physics*, Vol. 38, Pt. 1, No. 7B, 1999, pp. 4595–4600.

[29]Woskov, P., Hadidi, K., Borras, M., Thomas, P., Green, K., and Flores, G., "Spectroscopic Diagnostics of an Atmospheric Microwave Plasma for Monitoring Metals Pollution," *Review of Scientific Instruments*, Vol. 70, No. 1, 1999, pp. 489–492.

[30]Ohata, M., and Furuta, N., "Spatial Characterization of Emission Intensities and Temperatures of a High-Power Nitrogen Microwave-Induced Plasma," *Journal of Analytical Atomic Spectrometry*, Vol. 12, No. 3, 1997, pp. 341–347.

[31]Kunhardt, E., "Generation of Large-Volume, Atmospheric-Pressure, Nonequilibrium Plasmas," *IEEE Transactions on Plasma Science*, Vol. 28, No. 1, 2000, pp. 189–200.

[32]Passow, M., Brake, M., Lopez, P., McColl, W., and Repetti, T., "Microwave Resonant-Cavity-Produced Air Discharges," *IEEE Transactions on Plasma Science*, Vol. 19, No. 2, 1991, pp. 219–228.

[33]Gordon, S., and McBride, B., "Computer Program for Calculation of Complex Chemical Equilibrium Compositions and Applications: I. Analysis," NASA RP-1311, Oct. 1994.

[34]Gordon, S., and McBride, B., "Computer Program for Calculation of Complex Chemical Equilibrium Compositions and Applications: II. Users Manual and Program Description," NASA RP-1311, June 1996.

[35]Banwell, C., and McCash, E., *Fundamentals of Molecular Spectroscopy*, 4th ed., McGraw–Hill, London, 1994.

[36]Bernath, P., *Spectra of Atoms and Molecules*, Oxford Univ. Press, New York, 1995.

[37]Laher, R., and Gilmore, F., "Improved Fits for the Vibrational and Rotational Constants of Many States of Nitrogen and Oxygen," *Journal of Physical and Chemical Reference Data*, Vol. 20, No. 4, 1991, pp. 685–712.

[38]Krupenie, P., "The Spectrum of Molecular Oxygen," *Journal of Physical and Chemical Reference Data*, Vol. 1, No. 2, 1972, p. 423.

[39]Lique, J., and Crosley, D., "LIFBASE: Database and Spectral Simulation Program (Version 1.5)," SRI International Rept. MP 99-009, 1999.

[40]Chianese, S. G., and Micci, M. M., "Spectroscopic Emission Thermometry of the Microwave Arcjet Chamber Oxygen Plasma," AIAA Paper 2004-4125, July 2004.

[41]Chianese, S. G., "Microwave Electrothermal Thruster Chamber Temperature Measurements and Energy Exchange Calculations," Ph.D. Thesis, Dept. of Aerospace Engineering, Pennsylvania State Univ., University Park, PA, May 2005.